

Electronic Supplementary Information

Polymorphism and tautomeric preference in fenobam and the utility of NLO response to detect polymorphic impurity

Sajesh P. Thomas, K. Nagarajan and T.N. Guru Row*

Table of contents

No.		Page no.
1.	Methods of preparation of crystal forms of fenobam	2-3
2.	Crystallographic data table, crystal structure refinement details and ORTEP diagrams	3-5
3.	Inter and intra-molecular interactions	6
4.	Powder XRD patterns and details of profile fitting	7-11
5.	Second Harmonic Generation (SHG) measurements	11-12
6.	Computational details	12
7.	Infra-red spectra	13-14
8.	Thermal analysis	15-16

1. Methods of preparation of crystal forms of fenobam

The various crystallization conditions leading to five crystal forms of Fenobam:

Example	Solvent	Process/ condition of crystallization	Crystal form resulted
1*	a) Acetone-methanol b) THF-ether	Synthesized and filtered precipitate recrystallized from the solvents	Anhydrous “pure form”(now identified to be form III)
2*	a) DMF and stirring with water	the pure form was dissolved in DMF and added with excess of water, filtered and dried.	Monohydrate Form I
3	Water-ethanol (1:1 mixture)	synthesized and filtered form of the compound, recrystallized from Water-ethanol mixture	Monohydrate Form I
4	Water-methanol (1:1 mixture)	synthesized and filtered form of the compound, recrystallized from Water-methanol mixture	Monohydrate Form I
5	Non-solvent method	Monohydrate Form I, was heated at 80°-85°C for 2 hours	Form II
6	Non-solvent method	Monohydrate Form I, was heated at 100°C for 4 hours	Form III
6	ethanol	synthesized and filtered form of the compound, recrystallized from ethanol	Form III
7	methanol	synthesized and filtered form of the compound, recrystallized from methanol	Form III
8	acetic acid	synthesized and filtered form of the compound, recrystallized from acetic acid	Form III
9	acetone	synthesized and filtered form of the compound, recrystallized from acetone	Form III
10	Diethyl ether-ethanol	synthesized and filtered form of the compound, recrystallized from diethyl ether-ethanol mixture	Form III
11	DMSO	synthesized and filtered form of the compound, recrystallized from methanol	Form III
12	THF	synthesized and filtered form of the compound, recrystallized from DMSO	Form III

13	Water-methanol-triethylamine	synthesized and filtered form of the compound, recrystallized from water-methanol-triethylamine solutions of P ^H range (8-11).	Form III
14	acetonitrile-triethylamine	synthesized and filtered form of the compound, recrystallized from water-methanol-triethylamine solutions of P ^H range (8-11).	Form III
15	acetonitrile	synthesized and filtered form of the compound, recrystallized from acetonitrile	Form IV as a minor product concomitantly with Form III as the major product
16	acetonitrile (chiral seeding)	Monohydrate form I prepared by the process given example 1, recrystallized from acetonitrile in the presence of the seed crystals of L-ascorbic acid.	Hemihydrate form V as concomitant product with form I and form III

* 1 and 2 have been carried out following methods given by C. R. Rasmussen, U.S. Patent, 1976, 3983135.

2. Single crystal X-ray diffraction and crystal structure refinement

Single crystal X-ray diffraction data were collected on an Oxford Xcalibur Eos (Mova) Diffractometer using MoK α radiation ($\lambda=0.7107\text{ \AA}$) with X-ray generator operating at 50 kV and 1 mA.¹ The structures were solved and refinement was carried out using SHELX97² module in the program suite WinGX.³ The geometric calculations were carried out by PARST95 and PLATON.⁴ Molecular diagrams were generated using ORTEP-3⁵ and the packing diagrams were generated using Mercury 2.3.

Determination of the correct tautomeric structure: The hydrogen atom in question, the one attached to N3 has been located from a difference Fourier map of electron density in all the crystal structures. Other hydrogen atoms have been fixed from geometry and refined as riding atoms. In refinement of the structures form I and form IV the N3-H3 bond length has been refined with a restraint using DFIX command in SHELX97. The tautomeric structure thus assigned, is further validated by patterns of intermolecular interactions.

Twin refinement of form V: Crystals of form V are twinned and hence a two component twin reduction of the reflection data is carried out. The final refinement has been carried out using a reflection file of HKLF 5 format with BASF value of 0.48235 to account for twinning.²

1. Oxford Diffraction (2009). CrysAlis PRO CCD and CrysAlis PRO RED. Oxford Diffraction Ltd, Yarnton, England.
2. G. M. Sheldrick, Acta Crystallogr., Sect. A: 64(2008), p.112.
3. L. J. Farrugia, J. Appl. Crystallogr., 32(1999), p.837.

4. A. L. Spek, J. Appl. Crystallogr., 36(2003), p.7.

5. L. J. Farrugia, J. Appl. Crystallogr., 30(1997), p.565.

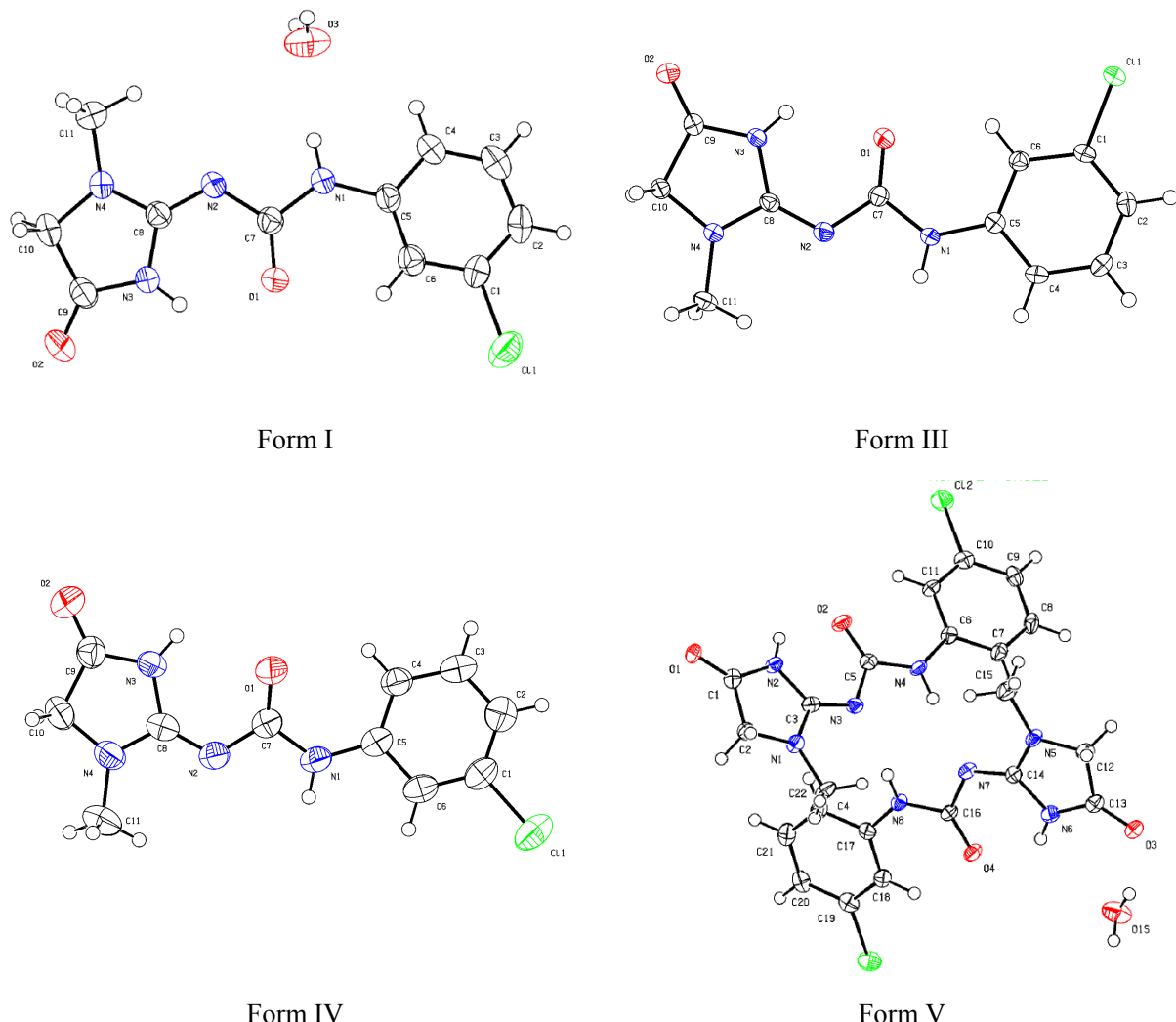


Figure S1. ORTEP of various forms of fenobam plotted with 50% probability ellipsoids and the atom numbering scheme.

Table S1. Crystallographic refinement details of crystal forms of fenobam

Data	Form I Monohydrate	Form III Anhydrous	Form IV Anhydrous	Form V Hemihydrate
Formula	C ₁₁ H ₁₁ ClN ₄ O ₂ .H ₂ O	C ₁₁ H ₁₁ ClN ₄ O ₂	C ₁₁ H ₁₁ ClN ₄ O ₂	(C ₁₁ H ₁₁ ClN ₄ O ₂) ₂ .H ₂ O
Formula weight	284.7	266.7	266.7	551.39
CCDC number	890752	890754	890755	890753
Temperature (K)	293 K	100 K	293 K	100 K
Crystal system	Triclinic	Monoclinic	Monoclinic	Triclinic
Space group	<i>P</i> -1	<i>Cc</i>	<i>P2/n</i>	<i>P</i> -1
<i>a</i> (Å)	7.7579(16)	12.8327(14)	9.8920(7)	9.8299(15)
<i>b</i> (Å)	8.6433(16)	7.6792(14)	9.5113(7)	11.4813(19)
<i>c</i> (Å)	10.536(2)	11.9725(14)	12.8459(9)	11.6916(15)
α (°)	92.620(16)	-----	-----	105.930(13)
β (°)	92.898(17)	101.188(9)	101.984(8)	97.779(12)
γ (°)	114.618(19)	-----	-----	104.196(13)
Volume (Å ³)	639.7(2)	1157.4(3)	1182.27(15)	1200.7(3)
<i>Z</i>	2	4	4	2
Density (gcm ⁻³)	1.478	1.531	1.498	1.525
μ (mm ⁻¹)	0.309	0.330	0.323	0.324
F (000)	296	552	552	572
<i>h</i> _{min, max}	-7, 9	-15, 15	-11, 11	-11, 11
<i>k</i> _{min, max}	-10, 10	-9, 9	-10, 11	-13, 13
<i>l</i> _{min, max}	-12, 12	-14, 14	-15, 15	-13, 13
No. of unique reflections	2255	2226	2084	6887
No. of parameters	209	168	164	367
<i>R</i> _{all} , <i>R</i> _{obs}	0.0644, 0.0496	0.0286, 0.0260	0.1159, 0.0641	0.1148, 0.0707
<i>wR</i> ₂ _{all} , <i>wR</i> ₂ _{obs}	0.1413, 0.1272	0.0620, 0.0606	0.1679, 0.1427	0.2150, 0.1924
$\Delta\rho_{\text{min,max}}$ (e Å ⁻³)	-0.296, 0.259	-0.201, 0.153	-0.243, 0.438	-0.446, 0.461
GOOF	1.077	1.021	1.005	1.052

Table S2. Relevant intra- and intermolecular interactions

Crystal	D-H···A	D-H/Å	D···A/Å	H···A/Å	∠D-H···A/°	symmetry
Form I	N3-H3···O1	0.84(2)	2.652(3)	2.07(2)	127 (2)	x,y,z
	N1-H1···O3	0.86	2.897(4)	2.04	170	x,y,z
	C6-H6···O1	0.93	2.863(3)	2.31	118	x,y,z
	O3-H3b···O1	0.72	2.943(4)	2.43	130	x+1,+y,+z
	O3-H3a···N2	0.87	3.007(3)	2.14	174	-x+1,-y+1,-z+1
	C2-H2···O2	0.93	3.520(4)	2.68	150	x+1,+y+1,+z+1
	O3-H3b···O2	0.72	3.128(4)	2.49	150	-x,-y,-z+1
	N3-H3···O2	0.84(2)	3.065(3)	2.39(2)	138 (2)	-x-1,-y,-z+1
	C11-H11b···Cl1	0.95	3.722(4)	2.90	145	-x,-y+1,-z+1
Form III	N3-H3A···O1	0.81(2)	2.679(2)	2.14(2)	124 (2)	x,y,z
	C6-H6···O1	0.93	2.891(2)	2.30	121	x,y,z
	N1-H1···O2	0.86	2.924(2)	2.09	165	x,-y+1,+z-1/2
	C4-H4···O2	0.93	3.366(2)	2.63	137	x,-y+1,+z-1/2
	C10-H10A···O1	0.97	3.686(2)	2.79	154	x+1/2,+y-1/2,+z
	C11-H11A···O2	0.96	3.776(2)	2.97	142	x,-y,+z-1/2
	C11-H11B···Cl1	0.96	3.250(2)	2.95	100	x+1/2,-y+1/2+1,+z-1/2
Form IV	N3-H3···O1	0.84(3)	2.713(4)	2.32(4)	109(3)	x,y,z
	N3-H3···O1	0.84(3)	2.831(4)	2.00(3)	170(3)	-x+1/2+1,+y,-z+1/2+1
	C4-H4···O1	0.93	2.858(5)	2.29	118	x,y,z
	N1-H1···O2	0.86	3.051(4)	2.20	170	x-1/2,-y+1,+z-1/2
	C6-H6···O2	0.93	3.510(5)	2.80	134	x-1/2,-y+1,+z-1/2
	C10-H10B···N2	0.97	3.515(5)	2.64	151	-x+2,-y+1,-z+1
Form V	N2-H2N···O2	0.88(4)	2.669(5)	2.01(5)	131(4)	x,y,z
	N6-H6N···O4	0.85(4)	2.644(5)	2.04(3)	127(3)	x,y,z
	N8-H8N···N3	0.90	3.041(4)	2.14	178	x,y,z
	C11-H11···O2	0.93	2.892(6)	2.29	122	x,y,z
	C18-H18···O4	0.93	2.859(6)	2.26	122	x,y,z
	N4-H4N···N7	0.87	3.080(4)	2.21	171	x,y,z
	N6-H6N···O1S	0.85(4)	3.234(5)	2.74(3)	118(4)	x,y,z
	O1S-H2O···O3	0.90(8)	2.821(5)	1.97(7)	158(6)	x,y,z
	C4-H4A···O4	0.96	3.242(4)	2.55	129	-x+1,-y,-z+1
	C7-H7···O3	0.93	3.215(6)	2.51	133	-x+1,-y+1,-z+1
	C12-H12B···O1S	0.97	3.356(5)	2.55	141	-x+1,-y+1,-z+1
	C20-H20···O2	0.93	3.532(6)	2.70	149	-x+1,-y,-z+2
	C22-H22···O1	0.93	3.360(6)	2.67	132	-x+2,-y,-z+2
	O1S-H1O···O1	0.88(4)	2.814(4)	1.94(4)	174(4)	x-1,+y,+z-1

Powder X-ray diffraction and details of profile fitting

Powder X-ray diffraction data were collected on a Philips, X'pertPro powder diffractometer in reflection geometry using Cu as anode. Profile refinements (LeBail fit) were carried out using Jana2000 [1]. Profile parameters such as GU, GV, GW, LX and LY are refined using Pseudo-Voigt function, in such a way that the profile fits best with the experimentally observed PXRD pattern. The values of cell parameters, (a,b,c, and symmetry unrestricted angles (for e.g., in case of monoclinic system only beta angle) of the known phase are given as input which are further refined. This technique has been employed to examine the powder phases, as it is a superior way to check the phase purity than a simple peak matching. Any impurity, if present, will appear as a difference peak ($Y_{\text{obs}} - Y_{\text{calc}}$) indicative of the presence of a different phase.

The following representations are used in the powder X-ray diffractograms :- crosses: observed pattern, red line: fitted profile, black line: difference curve between observed and calculated profiles($Y_{\text{obs}} - Y_{\text{calc}}$), tick marks: reflection positions.

[1] V. Petricek, M. Dusek and L. Palatinus, Jana2000, 08/11/2007 ed., 2007.

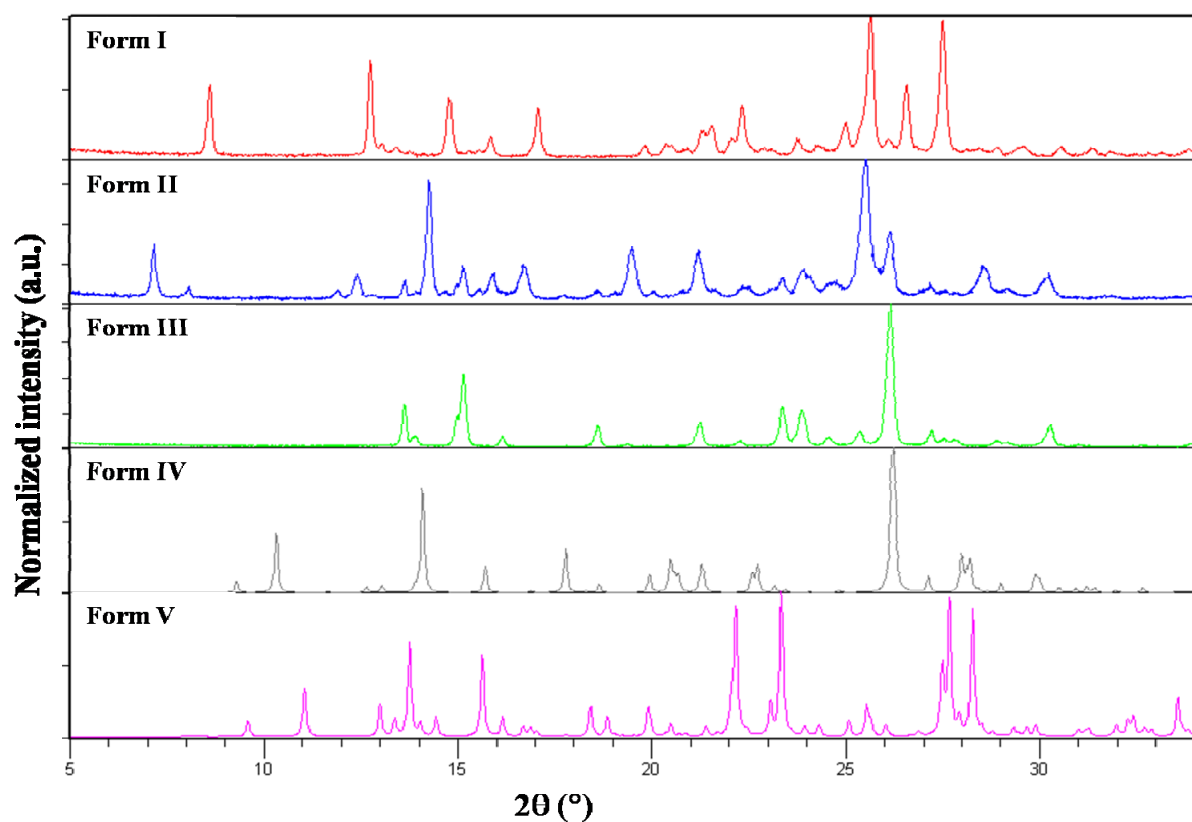


Figure S2. PXRD patterns of the five crystal forms of fenobam.

(1) Phase analysis by powder X-ray diffraction and profile fitting

Fenobam monohydrate (form I) loses water molecule upon heating above 80 °C and transforms into an anhydrous phase (form II). A profile refinement of the PXRD pattern of form II, carried out with the input cell parameters of form I suggest that form II is significantly different from form I (Figure S1). This intermediate form further transforms to anhydrous form (form III) above 90 °C. This has been further confirmed by profile fitting with the cell parameters of form III obtained from single crystal data (Figure S3). However, indexing of this intermediate phase could not be attempted due to the presence of peaks overlapping with form I and form III.

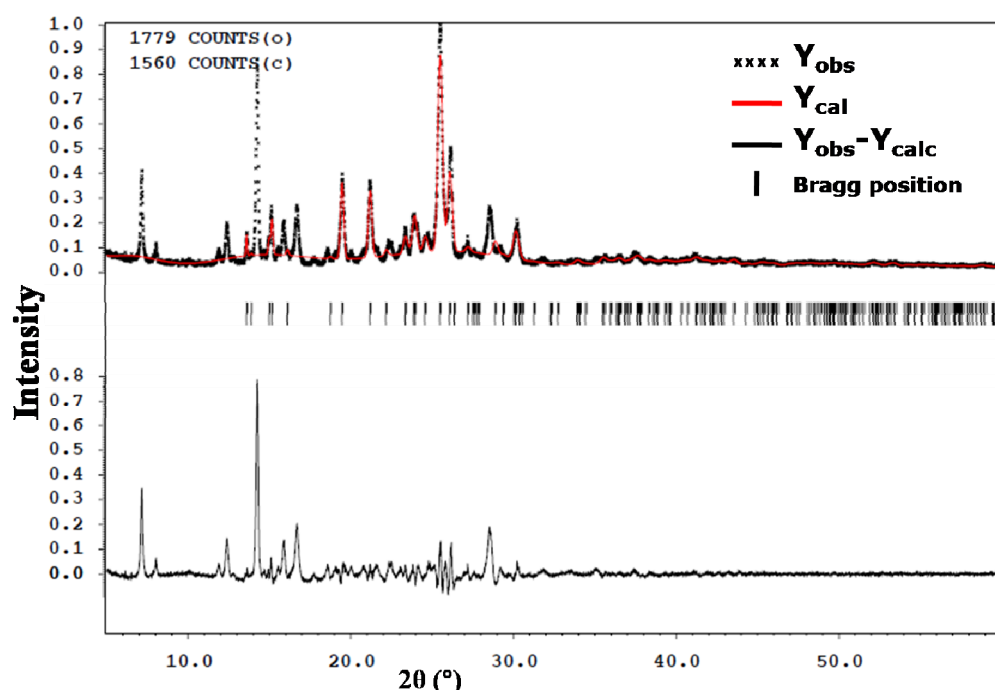


Figure S3. Profile fitting refinement of the phase obtained after heating form I at 85 °C. The input cell parameters of form I are used for the calculation of profile. The difference curve suggests the formation of a new phase (form II).

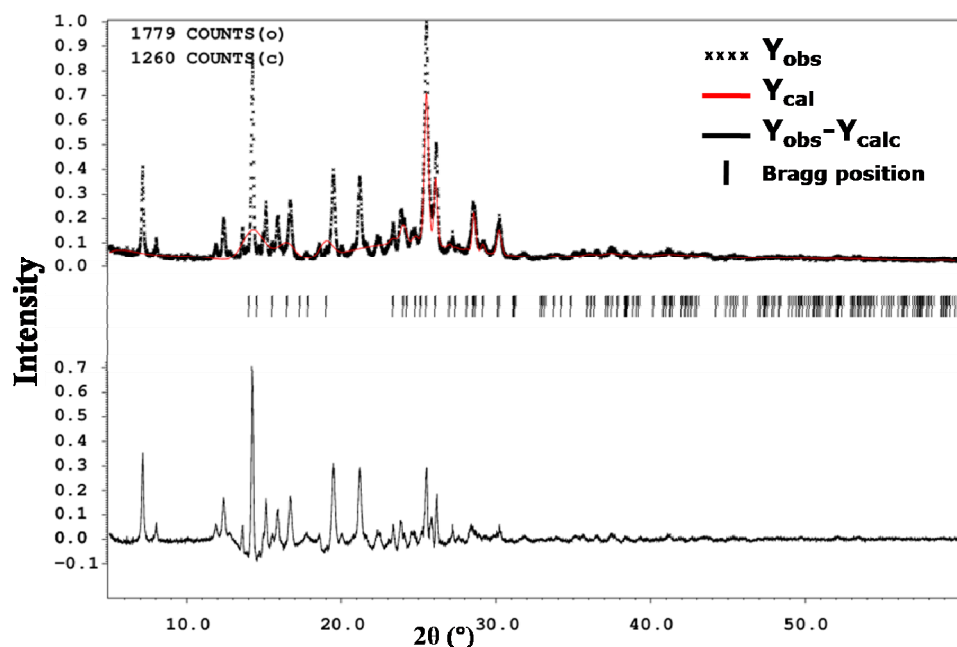


Figure S4. Profile fitting refinement of the phase (form II)obatined after heating form I at 85 °C. The input cell parameters of form III are used for the calculation of profile.

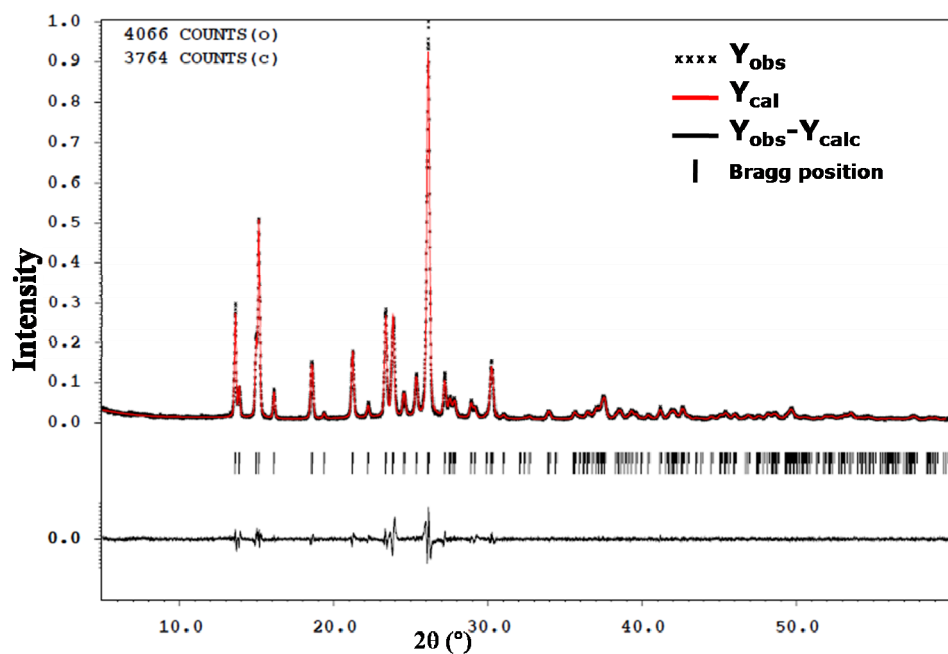


Figure S5. Profile fitting refinement of the phase obatined after heating form I at 100 °C. The input cell parameters of form III are used for the calculation of profile.

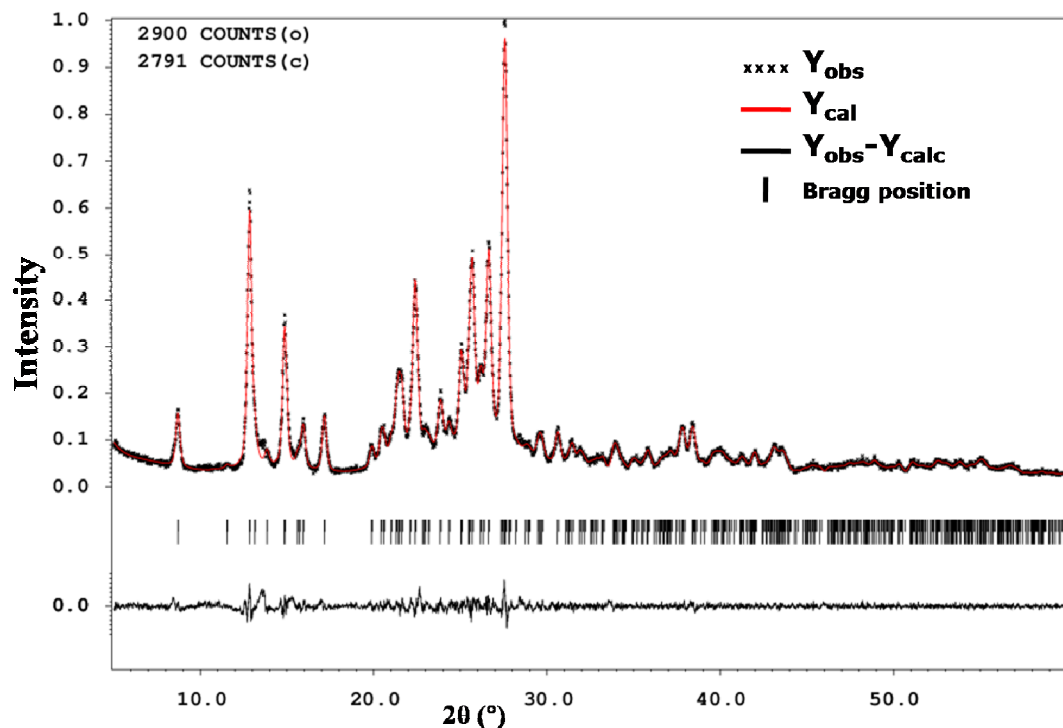


Figure S6. PXRD pattern of fenobam form I mixed with 5 % polymorphic impurity of form III.

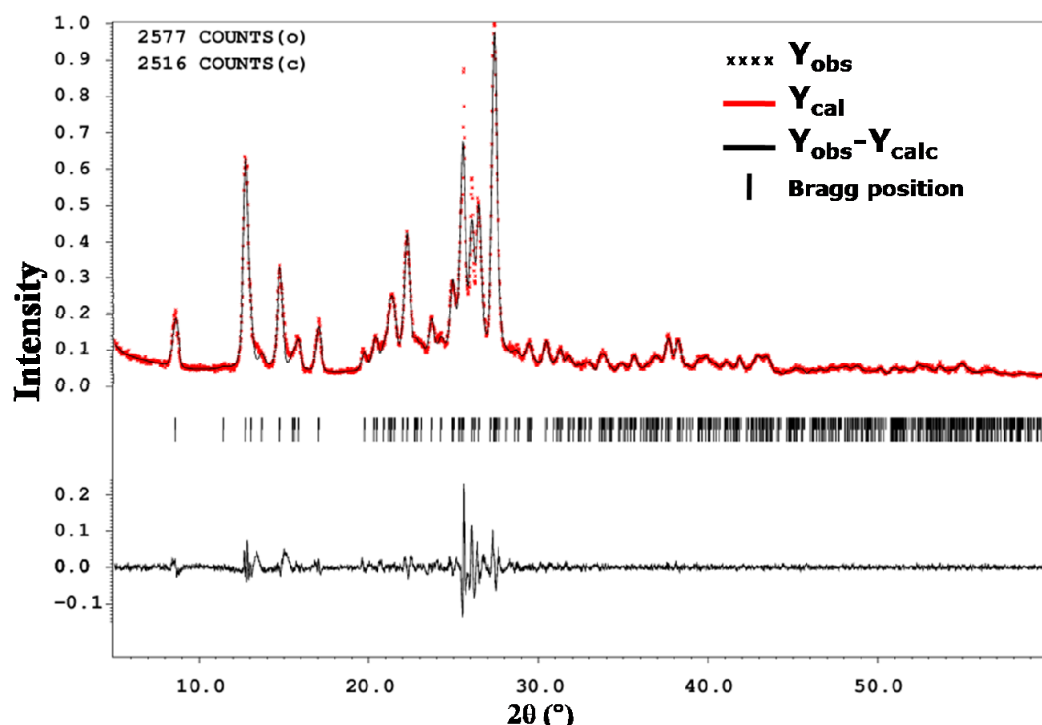


Figure S7. PXRD pattern of fenobam form I mixed with 10 % polymorphic impurity of form III.

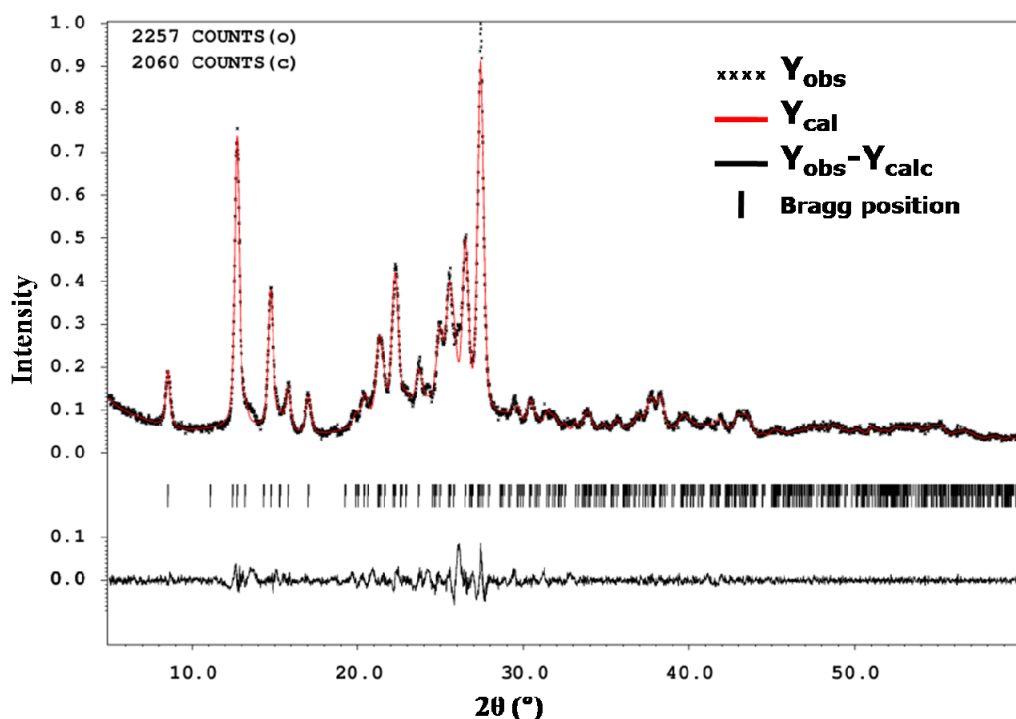


Figure S8. PXRD pattern of fenobam form I mixed with 20 % polymorphic impurity of form III.

Second Harmonic Generation (SHG) measurements

SHG measurements were carried out following Kurtz-Perry method on the powdered samples of the fenobam crystal forms at room temperature. For the light source for SHG experiment, a Q-switched Nd:YAG laser of fundamental wavelength 1064 nm (pulse width of 10 ns and repetition rate of 10 Hz; Spectra Physics, PROLAB 170) was used. The laser beam was passed through a couple of high energy laser mirrors (99.9% reflection, Melles Griot) and a glass filter (RG 645, to reject the light from the flash lamp of laser) before focusing. The input beam energy of the laser was 4.4 mJ /pulse. The incident beam power was measured using a power meter (Scientech Vector H410). The beam was focused using a converging lens of 200 mm focal length, into a glass capillary. The incoherently scattered SH photons were collected using a combination of a monochromator (Triax 550, Jobin Yvon, 0.024 nm resolution, 5 mm entrance and exit slit widths) and a photomultiplier tube (Hamamatsu, R2059) in the transverse direction. The second harmonic signal was then sampled, and recorded in a digital storage oscilloscope (Tektronix TDS 3520B). The SHG signals observed for the various samples and the reference samples of urea and KDP (potassium dihydrogen phosphate) are given in table S3.

The samples have been prepared by mixing weighed samples of form I and form III in the respective proportions followed by thorough grinding. The results suggest that there is significant increase in the SHG signal with increase in polymorphic impurity content. The results have been reproduced to confirm the low percentage impurity detection. Though the trend of

increasing SHG signal with increasing impurity level is reproducibly observed no linear correlation could be derived between the two. It is to be noted that the absolute value of SHG efficiency is susceptible to variations with respect to the method of measurement, particle size of the sample and the tightness of sample packing.

Table S3. SHG signals obtained by Kurtz-Perry method

Input beam energy = 4.4 mJ/pulse	NLO response
Urea	166 mV
KDP (Potassium dihydrogen phosphate)	14.9 mV
Fenobam , form III	320 mV
Fenobam, form I	0 mV
Physical mixture of 3% III and 97% I	17.6 mV
Physical mixture of 5% III and 95% I	19.2 mV
Physical mixture of 10% III and 90% I	21 mV
Physical mixture of 15% III and 85 % I	55 mV
Physical mixture of 20% III and 80% I	68 mV

Computational details:

Gas phase optimization calculations have been carried out on fenobam with an input molecular structure as obtained from the single crystal data and with a basis set of b3lyp/6-311g(2df,2p)using Gaussian 03. The sketches of the frontier molecular orbitals (HOMO and LUMO)have been plotted using Chemcraft version 1.6. Further, the Hartree Fock energies of the two possible tautomeric forms of the molecule are compared, with two tautomeric structures as the input, followed by an optimization. Tautomer 1 with an intra-molecular N-H···N hydrogen bond has the energy value, HF=-1255.779493. Tautomer II with a molecular conformation stabilized by an intramolecular N-H···O hydrogen bond has the energy value, HF=-1255.792967. Hence the tautomeric structure II is found to be stabilized by an energy difference of 0.0134744 Hartrees or 8.45532 Kcal/mol.

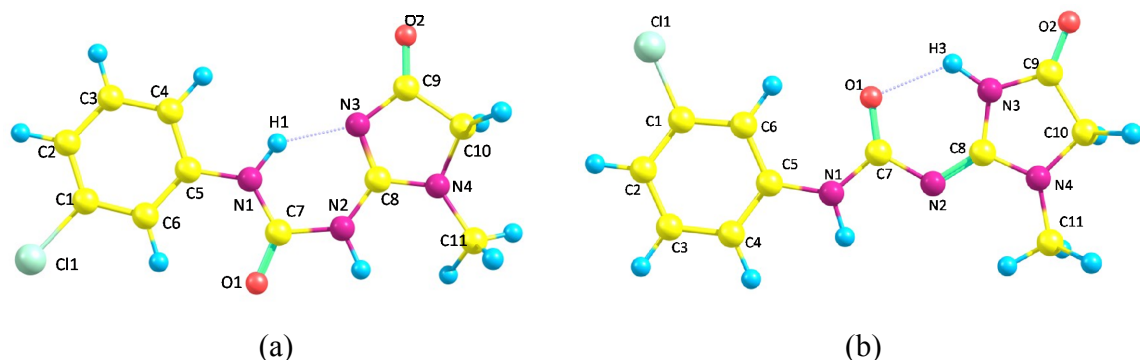


Figure S9. The optimized geometries of (a) tautomeric structure I with intra-molecular N-H···N hydrogen bond and (b) tautomeric structure II with intra-molecular N-H···O hydrogen bond.

FT-IR spectroscopy

Fourier transform infrared (FTIR, Perkin-Elmer FTIR Spectrometer Spectrum 1000) spectra were recorded on the different polymorphs with requisite amount of the crystalline sample added to spectroscopic grade KBr and pressed to form pellets with diameter and thickness equal to 12 mm and 1 mm, respectively. The characteristic absorption bands are expressed in cm^{-1} .

FT-IR spectrum of form **I** is characterized by the following peaks:

3592, 3416, 3296, 2358, 1752, 1639, 1533, 1421, 1315, 1209, 1132, 1005, 779, 723, 575 cm^{-1} .

FT-IR spectrum of form **III** is characterized by the following peaks:

3590, 3415, 3288, 2365, 1752, 1632, 1526, 1414, 1315, 1209, 1132, 999, 779, 716, 575 cm^{-1} .

It is to be noted that from the FT-IR spectrum mixture of form I and III, it is not possible to infer the presence of any impurity phase (Figure S10).

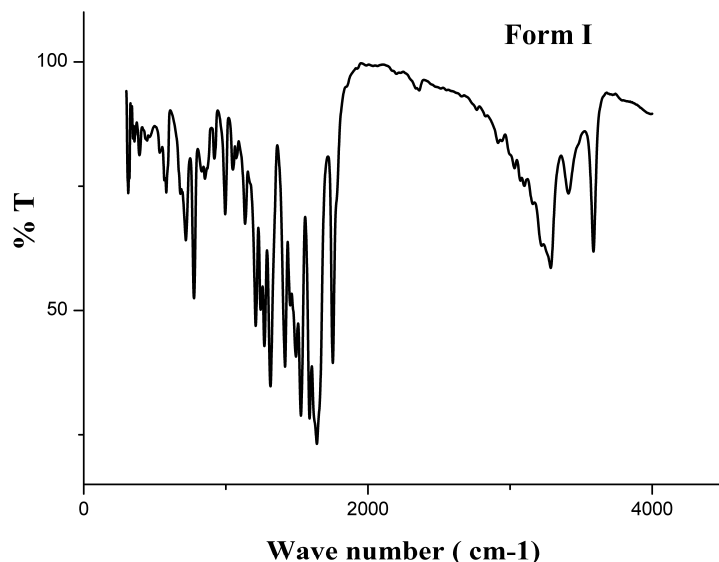


Figure S10. FT-IR spectra of hydrated form **I** of fenobam.

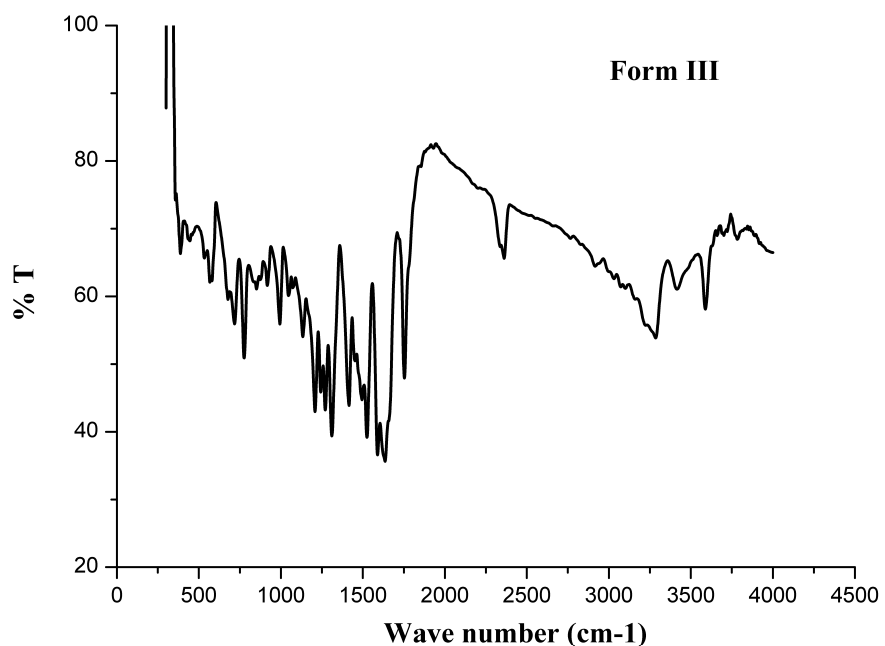


Figure S11. FT-IR spectra of hydrated form III of fenobam.

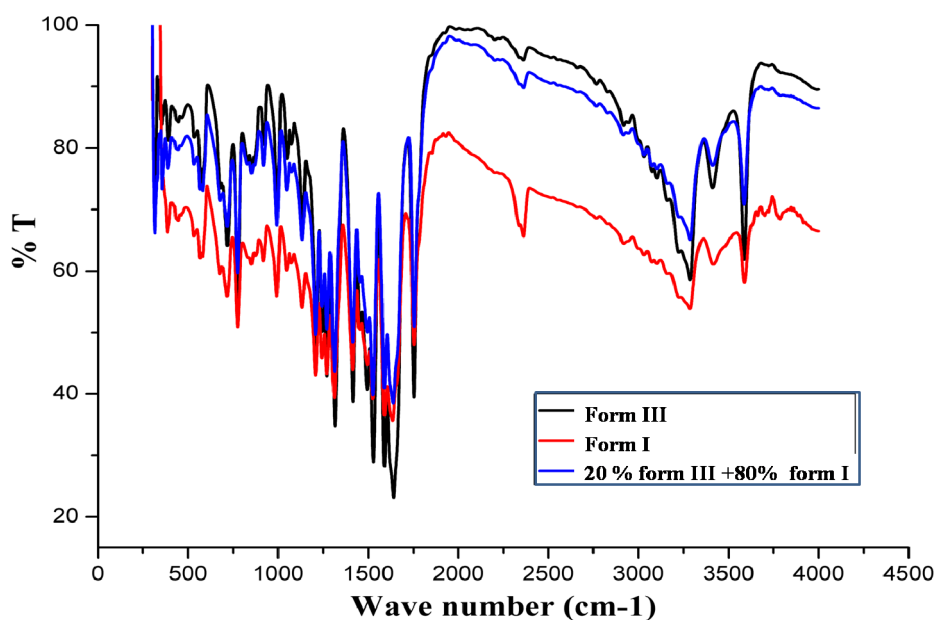


Figure S12. FT-IR spectra of the mixture of form I and impurity phase form III (20%).

Differential scanning calorimetry (DSC) and thermo gravimetric analysis (TGA):
Differential scanning calorimetry (Mettler Toledo STAR) studies and thermo gravimetric analysis (Mettler Toledo) were carried out over a temperature range of 25–300 °C with a ramp rate of 5 °C/min.

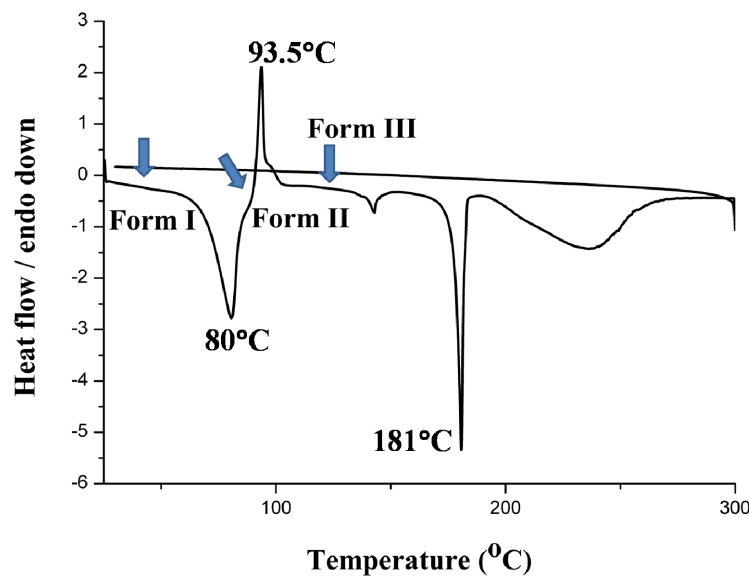


Figure S13. Differential scanning calorimetric (DSC) thermogram of hydrated form I of fenobam.

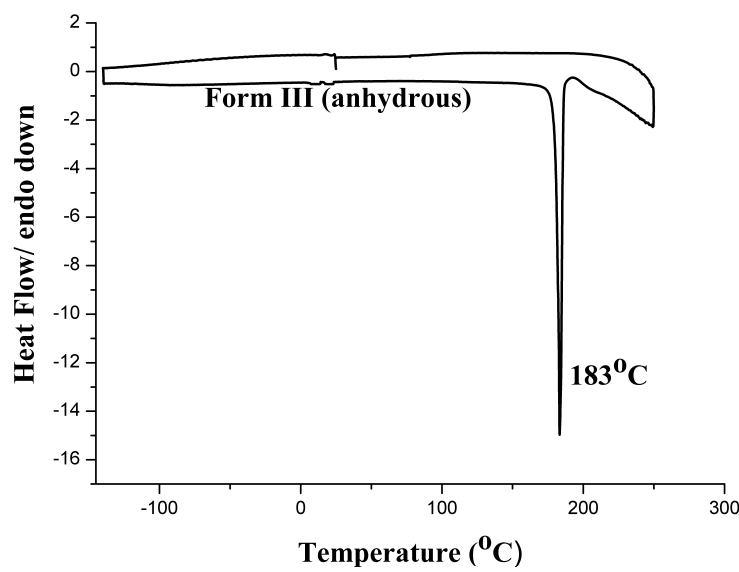


Figure S14. Differential scanning calorimetric (DSC) thermogram of anhydrous form III crystals of fenobam grown from solvent evaporation at room temperature.

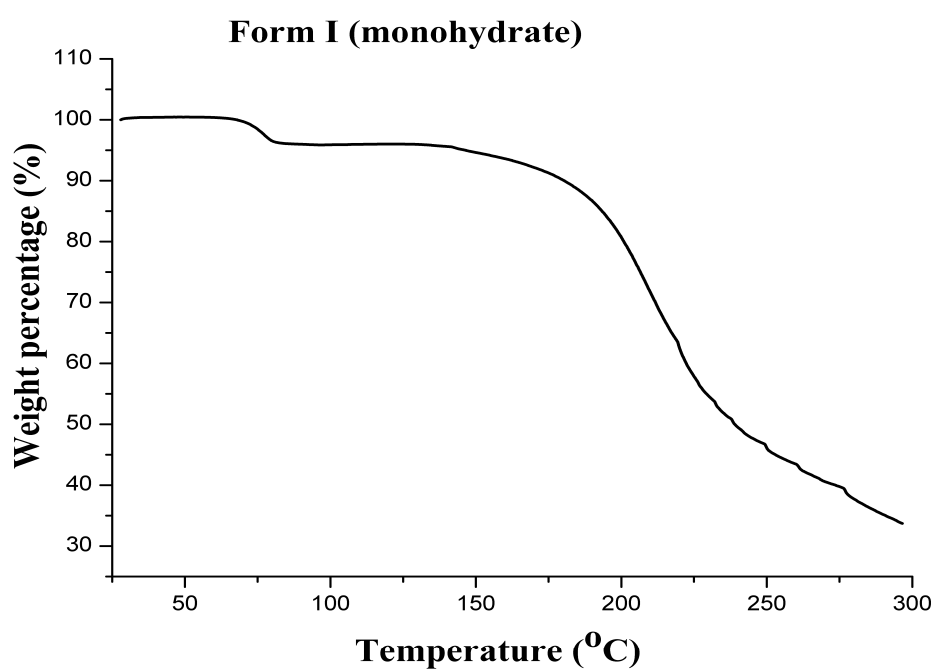


Figure S15. Thermo gravimetric analysis (TGA) of hydrated form I of fenobam.

Crystal data: Form I (monohydrate): $C_{11}H_{11}ClN_4O_2 \cdot H_2O$, Mr=284.7, triclinic, $P\bar{1}$, $a=7.7579(16)$ Å, $b=8.6433(16)$ Å, $c=10.536(2)$ Å, $\alpha=92.620(16)$, $\beta=92.898(17)$, $\gamma=114.618(19)$, $V=639.7(2)$ Å³, Z=2, T=293 K, $\rho_{\text{calc}}=1.478$ g cm⁻³, $R_{\text{obs}}=0.0496$, $R_{\text{all}}=0.0644$, G.o.F=1.077.

Form II: characterized by PXRD unique peaks.

Form III: $C_{11}H_{11}ClN_4O_2$, Mr=266.7, Monoclinic, Cc , $a=12.8327(14)$ Å, $b=7.6792(14)$ Å, $c=11.9725(14)$ Å, $\beta=101.188(9)$, $V=1157.4(3)$ Å³, Z=4, T=100 K, $\rho_{\text{calc}}=1.531$ g cm⁻³, $R_{\text{obs}}=0.0260$, $R_{\text{all}}=0.0286$, G.o.F=1.021.

Form IV: $C_{11}H_{11}ClN_4O_2$, Mr=266.7, Monoclinic, $P2/n$, $a=9.8920(7)$ Å, $b=9.5113(7)$ Å, $c=12.8459(9)$ Å, $\beta=101.984(8)$, $V=1182.27(15)$ Å³, Z=4, T=293 K, $\rho_{\text{calc}}=1.498$ g cm⁻³, $R_{\text{obs}}=0.0641$, $R_{\text{all}}=0.1159$, G.o.F=1.005.

Form V (hemihydrate): $(C_{11}H_{11}ClN_4O_2)_2 \cdot H_2O$, Mr=551.39, Triclinic, $P\bar{1}$, $a=9.8299(15)$ Å, $b=11.4813(19)$ Å, $c=11.6916(15)$ Å, $\alpha=105.930(13)^\circ$, $\beta=97.779(12)^\circ$, $\gamma=104.196(13)^\circ$, $V=1200.7(3)$ Å³, Z=2, T=100 K, $\rho_{\text{calc}}=1.525$ g cm⁻³.